Development of Seismic Response Analysis Code of Cask

K.Shirai[1)], *C.Ito*[1)], *H.Ryu*[2)]

1) Central Research Institute of Electric Power Industry, 2) Maeda Corporation, Japan

INTRODUCTION

Since a cask is vertically oriented during loading in cask-storage, it is necessary to investigate the integrity of the cask against tip-over during strong earthquakes. The rocking and sliding behavior of the cask during strong earthquakes can be analyzed as a dynamic vibration problem for a rigid cylinder. (Mochizuki et al. 1948)

In this paper, in order to clarify the tip-over characteristics of a cask during strong earthquakes, we applied the Distinct Element Method (DEM) to the seismic response analysis of the cask. (Shirai et al. 1992) DEM was introduced by Cundall P.A. in 1971.
It is based on the use of an explicit numerical scheme. The cask was considered to be a rigid polygonal element, which satisfied the equation of motion and the law of action and reaction. We examined the applicability of this code by comparison with experimental results obtained from shaking table tests using scale model casks considering the dimension of a 100 tons class full-scale cask.

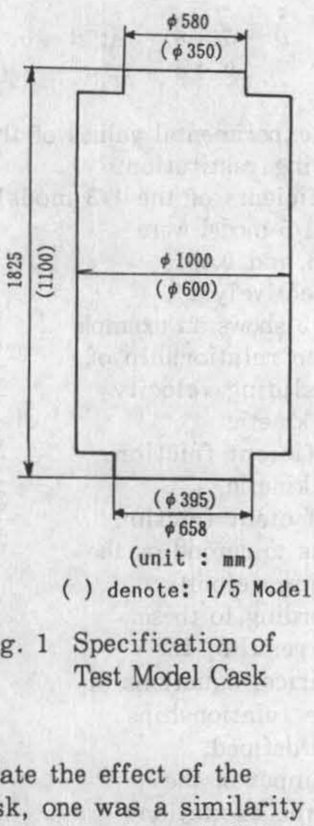

Fig. 1 Specification of Test Model Cask

SHAKING TABLE TEST

Description of Test

Fig. 1 shows the specifications of the two model casks. To simulate the effect of the gravitational acceleration on the tipping-over condition of the cask, one was a similarity model cask. The similarity law governing the model cask was summarized as shown in Tab. 1. The scaling ratio was set at 1/3 (1/3 model cask). Total weight was 12.6 tons and lead weights were applied to control the equivalent mass density in order to satisfy the similarity of the mass density. The other one was a scale effect model.
The scaling ratio was set at 1/5 (1/5 model cask) and total weight was 2.9 tons. As a model floor, a 45 cm thick reinforced concrete slab was used. Fig. 2 shows the shaking table test apparatus. A model cask and a model floor were fabricated on the shaking table. The shaking table excitation test was conducted using a one-dimensional earthquake simulator at Abiko Research Laboratory of CRIEPI (Chiba, Japan). During the shaking table

excitation test, the rotational angle, the angular velocity and sliding displacement of the cask were measured.

Before the shaking table test, the rocking restitution coefficient and kinetic coefficient friction between the model cask and the model floor were measured. The rocking restitution coefficient was assumed to be the damping ratio of the maximum angular velocity obtained from a free vibration test. It is defined by equation (1).

$$\dot{\theta} \rightarrow \delta \times \dot{\theta} \quad \text{at } \theta = 0$$
$$(0 < \delta < 1) \qquad \cdots\cdots(1)$$

The experimental values of the rocking restitution coefficients of the 1/3 model and 1/5 model were 0.963 and 0.951, respectively.

Fig. 3 shows an example of the relationship of the sliding velocity and kinetic coefficient friction. The kinetic coefficient friction seems to depend on the sliding velocity. According to these test results, the empirical equations of these relationships were defined.

For input of the seismic excitation tests, a sinusoidal wave and El Centro (1940 Imperial Valley Earthquake) and Hachinohe wave (1963 Tokachioki Earthquake) were employed as a typical natural earthquake. Time scales of the input waves were scaled according to a similarity law shown in Tab. 1. The acceleration levels were varied according to the test conditions. In the case of sinusoidal wave excitation, the shaking table was first excited by high frequency waves until the behavior of the model cask seemed to be stable. Afterwards, the frequency and acceleration level were set to the aimed test condition, and the response of the model cask was measured after a stationary state.

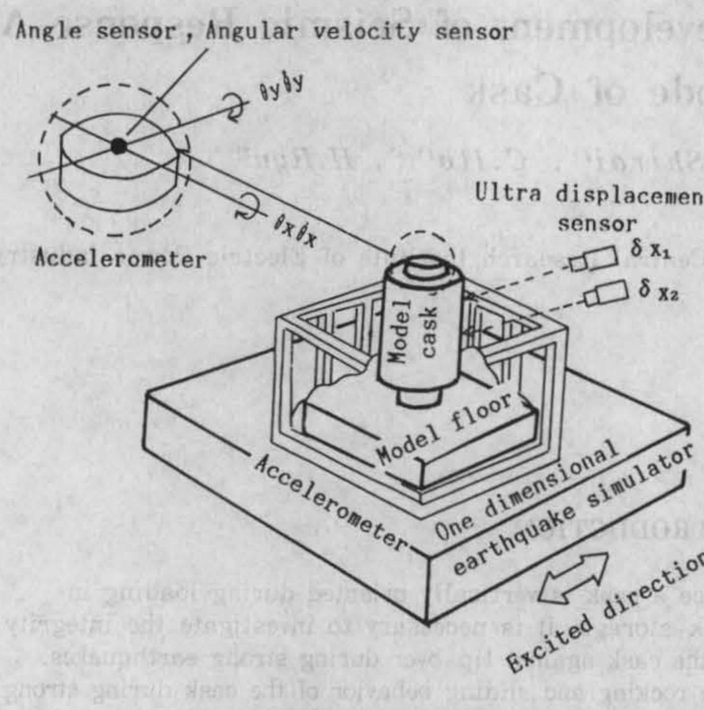

Fig. 2 Shaking Table Test

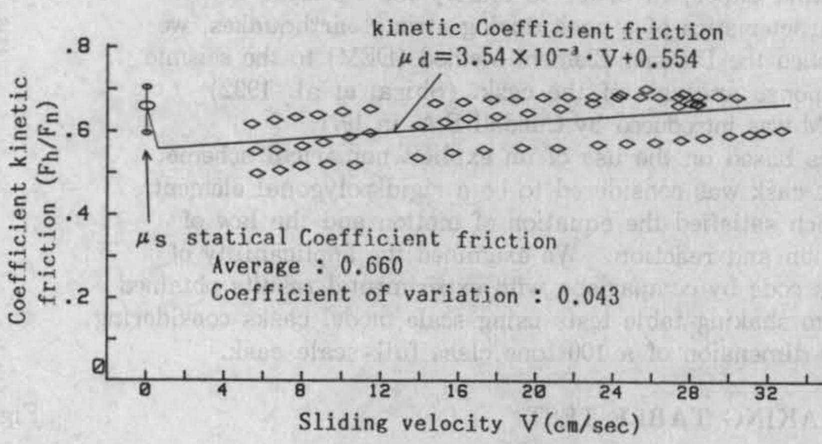

Fig. 3 Relationship of Sliding Velocity and Kinetic Coefficient Friction

Test Results

Fig. 4 shows the maximum values and lissajous curves of rotational angle response of the 1/3 model cask for sinusoidal wave excitation, which had an input displacement amplitude of 0.5 cm. A solid line shows theoretical solutions of the maximum rotational angle response of the two-dimensional rectangular blocks subjected to sinusoidal wave excitation considering a dimension of a model cask and an empirical value of the rocking restitution coefficient. (Ogawa 1980)

Although the test results show that three-dimensional behavior like top-spinning was observed, the test results were in good agreement with theoretical solution curves. Fig. 5 shows the maximum rotational angle response of a 1/3 model for natural earthquake waves. Since the dominant frequency of the Hachinohe wave was lower than the one for the El Centro wave, the response for Hachinohe wave excitation was bigger than the one for the El Centro wave excitation.

Tab. 1 Similarity Law

Parameter	Notation	Dimension	Similarity Ratio: General Form	Similarity Ratio: for N=3
Length	L	L	$L_m/L_p=1/N$	1/3
Weight	W	MLT^{-2}	$W_m/W_p=1/N^3$	1/9
Time	T	T	$T_m/T_p=1/\sqrt{N}$	1/1.73
Velocity	V	LT^{-1}	$V_m/V_p=1/\sqrt{N}$	1/1.73
Acceleration	A	LT^{-2}	$A_m/A_p=1$	1
Mass	M	M	$M_m/M_p=1/N^3$	1/9
Moment of Inertia	I	ML^2	$I_m/I_p=1$	1
Surface Force	P	$ML^{-1}T^{-2}$	$P_m/P_p=1$	1

(Note) Suffix p denotes the prototype, and suffix m denotes the model

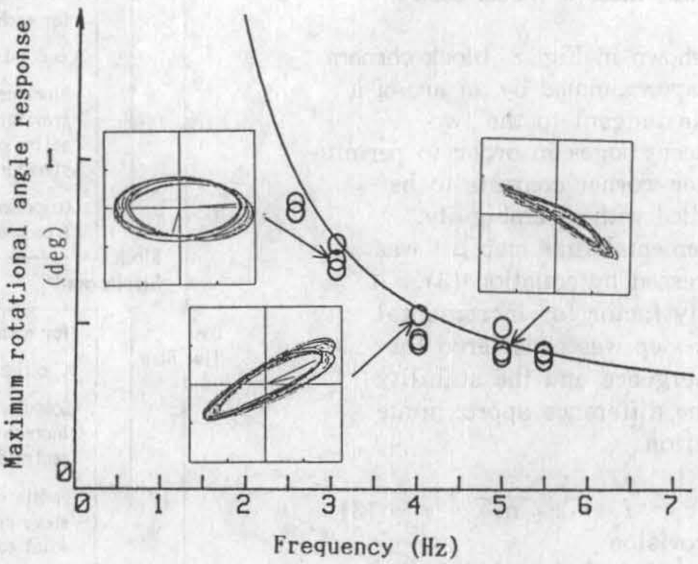

Fig. 4 Test Results for Sinusoidal Wave Excitation

ANALYTICAL EVALUATION BY DEM COMPUTER CODE

Description of Analysis Computer Code

We applied DEM to the seismic response analysis computer code. In DEM analysis, a medium is treated as a rigid block assemblage, and the block is assumed to be polygonal. The behavior of the individual rigid blocks is under the control of Newton's second law. The solutions to the equations of motion are obtained through a central difference scheme. Fig. 6 shows the outline of the calculation flow. The deformability of the discontinuities or interfaces between blocks and the frictional characteristics are represented by spring-slider systems located at contact points between blocks. As shown in Fig. 7, the acting force is divided at the contacting plane into two components a compressional force acting in the normal direction and a shear force acting in a tangential direction. The acting force between blocks is calculated by the amount of penetration between two adjacent blocks which can be defined directly from block geometry and block centroid translation and rotation. Shear forces are considered to be the frictional forces which are limited by a Mohr-Coulomb friction law. Rayleigh damping is applied to damping, and only a stiffness damping term is considered. It is expressed as equation (2).

$$[C]=\beta[K],\quad h=2\omega\cdot\beta \cdots\cdots (2)$$

provision

$\omega=\sqrt{k/m}$,

k : spring constant stiffness

m : mass of model cask

As shown in Fig. 8, block corners are approximated by an arc of a circle tangent to the two adjacent edges in order to permit corner-corner contacts to be handled without ambiguity. Incremental time step Δt was expressed by equation (3). A safety factor for incremental time step was considered for convergence and the stability of the difference approximate solution.

$$\Delta t = f_s \cdot 2\sqrt{m/k} \cdots\cdots\cdots (3)$$

provision

f_s : Safety factor (0.01)

Analysis Model

Fig. 9 shows the DEM analysis model. A model cask and model floor were represented as a convex polygon and assumed to be rigid in the two-dimensional plane. Shaking excitations were applied at the model floor. The radius of the bottom side of the analysis model was set to be equivalent to the radius of gyration around the edge of the bottom side of the model cask used in the shaking table test. The spring constant was determined from the spring restoring forces using

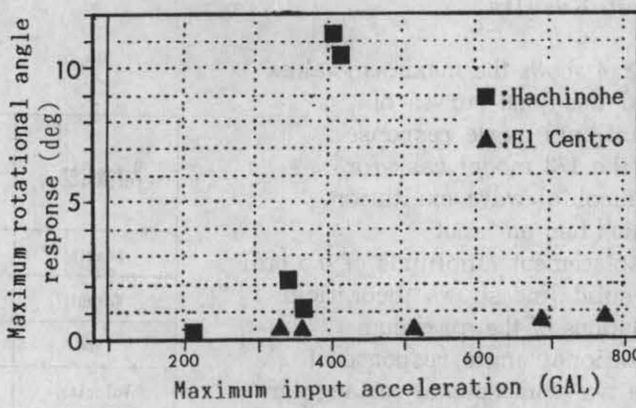

Fig. 5 Test Results for Natural Earthquake Wave Excitation

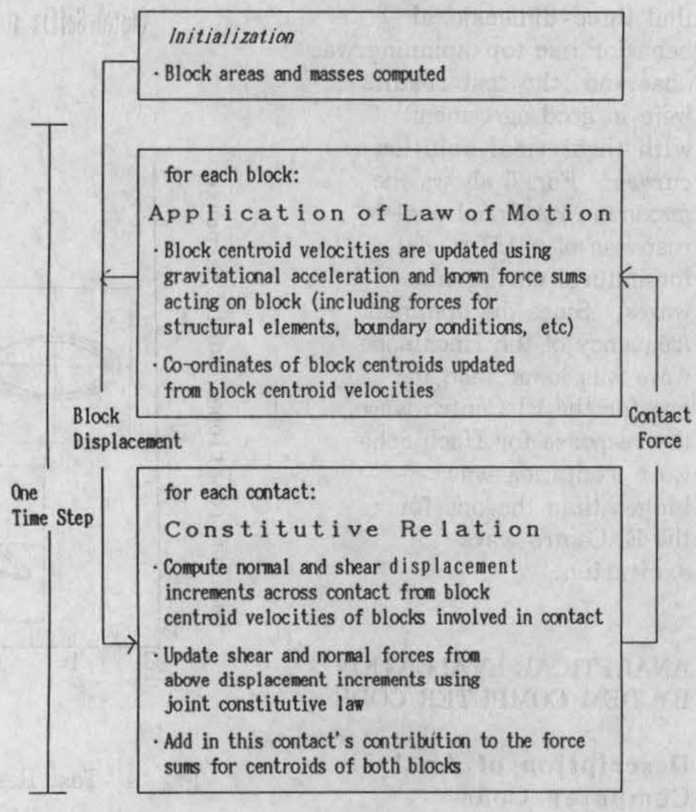

Fig. 6 Diagram Showing the Overall Calculation Flow of the DEM Code

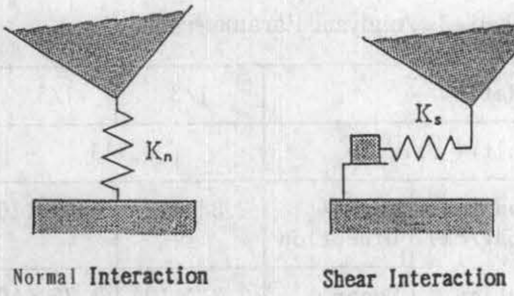

Fig. 7 Spring-slider System Located at Contact Point between Blocks

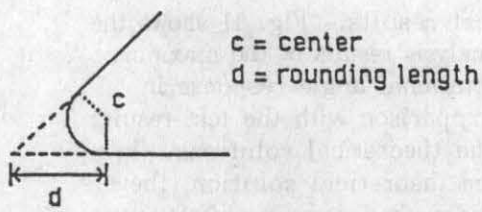

Fig. 8 Block Corners

Tab. 2 Spring Constant

	Spring Constant (Barkkan:1962)
Normal Direction	$K_n = G \cdot \beta_Z \cdot a / (1 - \nu)$
Shear Direction	$K_S = 2(1 + \nu) G \cdot \beta_X \cdot a$

ν : Poisson's Ratio β_Z:2.1
G : Shear Elastic Coefficient β_X:1.0

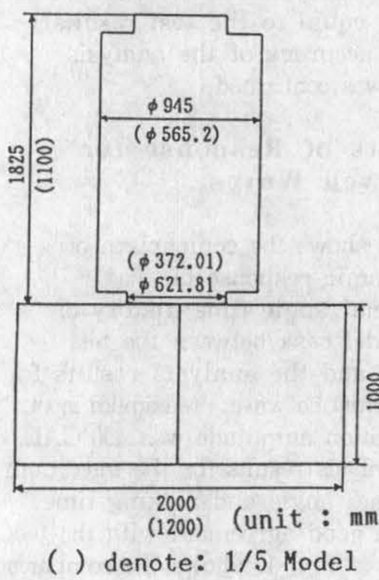

Fig. 9 DEM Analysis Model

a rectangular footing on the half-infinite elastic ground as shown in Tab. 2. (Barkan 1948)
It can be considered that the energy dissipation mainly occurs at the moment of the impact. So, for the rocking restitution coefficient, the damping value of the angular velocity obtained from free vibration testwas applied. The analysis damping ratio "h" was obtained by trial and error, so that the damping value obtained from free vibration analysis using Rayleigh damping was the same as the one obtained from test results. The rocking restitution coefficients of the 1/3 model and the 1/5 model obtained from the free vibration analysis were 0.964 and 0.948, respectively.
It was found that the kinetic coefficient friction depends on the sliding velocity, so in the analysis the empirical equation of the coefficient friction was applied as shown in Fig. 3. The analysis parameters were summarized in Tab. 3.

ANALYSIS RESULTS

Results of Responses for Sinusoidal Waves

The rocking analysis of the model cask was performed for sinusoidal waves when the input maximum displacement amplitude was constant. The input maximum displacement amplitude was set to 0.5 cm, 1.0 cm, and 1.5 cm. Fig. 10 shows the comparison of the time history of the rotational angle response between the test results and the analysis results using the 1/3 model. The input maximum displacement amplitude was 1.0 cm and excitation frequency was 4.0 Hz. The analysis results were in good agreement with the test results. Fig. 11 shows the analysis results of the maximum rotational angle response in comparison with the test results and theoretical solutions. In the theoretical solution, the sliding and damping effect were ignored. So, the analysis results were somewhat smaller than the theoretical solutions, but the analysis results were almost equal to the test results. So the accuracy of the analysis model was confirmed.

Results of Response for Observed Waves

Fig. 12 shows the comparison of the seismic response of rotational angle time history of the model cask between the test results and the analysis results for the Hachinohe wave. Maximum input acceleration amplitude was 400 GAL. The analysis results for the maximum rotational angle and rocking time were in good agreement with the test results. Fig. 13 shows the comparison of the results of the maximum rotational angle of the model cask between the test results and the analysis results for the Hachinohe wave using the 1/3 model and the 1/5 model. The analysis results were in good agreement with the test results.

CONCLUSION

In this study, we improved the two-dimensional DEM code and applied this scheme to the seismic response analysis of the cask, and the shaking table tests were performed using the model casks.

Following the results of the shaking table test and analysis, the outline of the contents and results is summarized below.

Tab. 3 Analysis Parameters

Scaling Ratio		1/3	1/5
Mass Density(g/cm³)		8.743	
Spring Constant (bar/cm)	Normal Direction	2.38×10^3	4.07×10^3
(distribution spring)	Shear Direction	2.21×10^3	3.76×10^3
Safety Factor of Time Step		0.01	
Rounding Length (cm)		0.50	
Coefficient Friction		Reference Fig.3	
Damping Ratio (%) (characteristic Frequency)		5.6 (135Hz)	5.6 (220Hz)

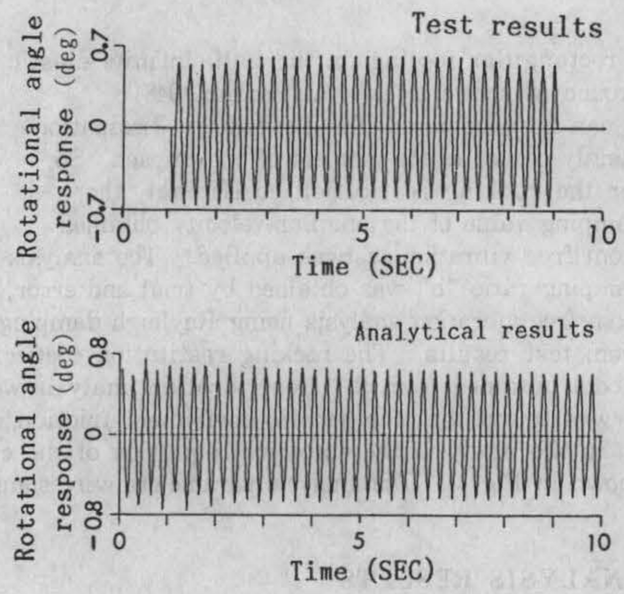

Fig. 10 Time History of Rotational Angle Response for Sinusoidal Wave Excitation

(1) For the sinusoidal wave, the test results were in good agreement with the two-dimensional theoretical solutions, and it was found that the tip-over behavior of the cask can be estimated with a two-dimensional plane problem. Moreover, the analysis results agreed with theoretical solutions. So, the accuracy of the analysis model was confirmed.

(2) For natural earthquake waves, the analysis results of maximum rotational angle, rocking time, and scale effect agreed with the test results. As a result, the seismic analysis computer code using DEM can accurately estimate tip-over behavior of the cask during strong earthquakes.

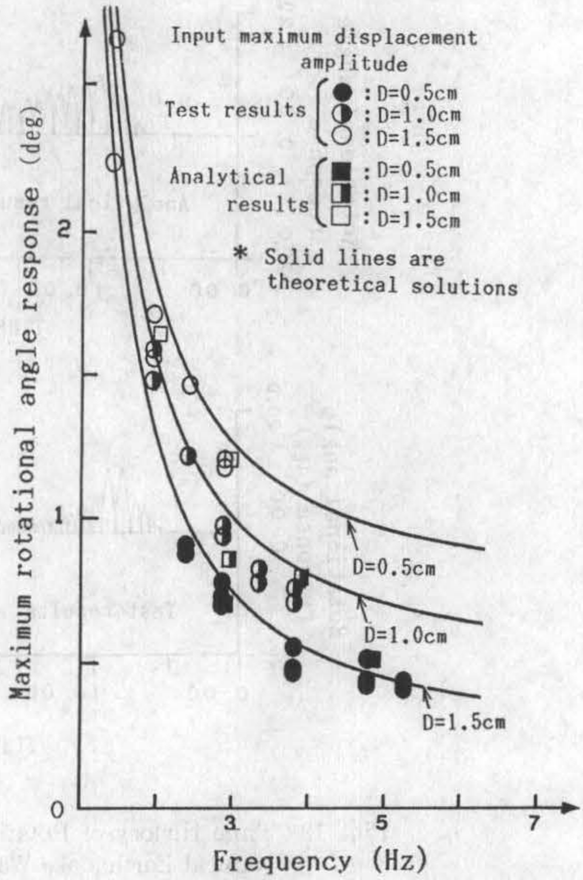

Fig. 11 Maximum Rotational Angle Response for Sinusoidal Wave Excitation

REFERENCES

Barkan, D.D., 1948, Dynamics of bases and foundation, McGraw Hill.

Mochizuki T. and K.Kobayashi, 1976, study on the acceleration of earthquake motion deduced from the movement of columns, Transaction of the Architectural Institute of Japan, Vol.248, 63-70 (in Japanese)

Ogawa N., 1980, Study on the overturning vibration of a rigid Structure, Transaction of the Architectural Institute of Japan, Vol.287, 51-63 (in Japanese)

Shirai K. and H.Ryu, 1992, Application of distinct element method for tipping-over casks, Proc. of Symposium on Computational Method in Structural Engineering and Related Fields Vol.16, 63-68 (in Japanese)

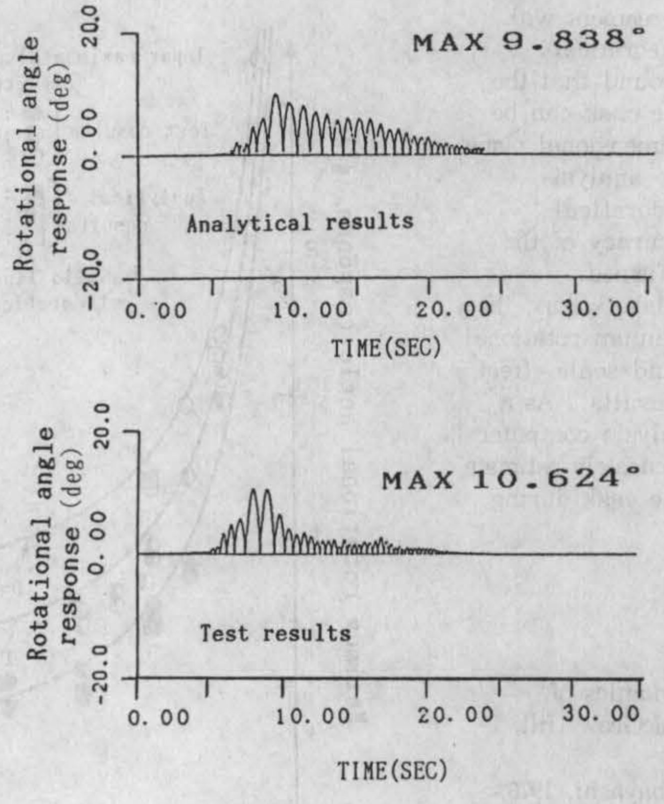

Fig. 12 Time History of Rotational Angle Response for Natural Earthquake Wave Excitation

(Input wave : Hachinohe, Acc. level; 400GAL)

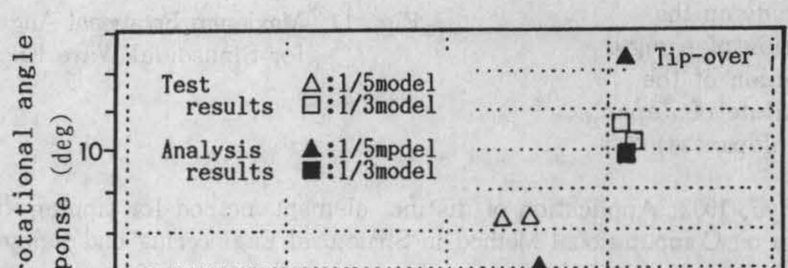

Fig. 13 Comparison of Test and Analysis for Scale Effect (Input wave : Hachinohe)